Supplementary material for "Measurement of strain in InGaN/GaN nanowires and nanopyramids"

Analytic calculations done for calculating strain and composition were based on the model of the infinite, biaxially strained plane, normally used for the thin films. Elastic relaxation is assumed to occur only in the direction of the free surface – perpendicular to the film. For the core-shell nanowires this is often not the case, as the shell is also allowed to relax through the edges. However, we are dealing with the nanowires of exceptionally core, compared to the shell – width of the side facet is around 220 nm, which is ten times more than the thickest shell. Therefore, we assume, that biggest part of the shell will not be affected by the presence of the edges and will behave as the infinite plane. In order to underpin this assumption we performed finite element method (FEM) simulations with realistic NW geometries and used and compared the calculated results with the measurements. Afterwards, we compare the properties of the optimal FEM model with results of the analytic calculations based on the infinite plane model.

A 3D model of a nanowire (NW) was built using the geometry known from the SEM images. It consisted of the GaN core and the InGaN shell with a given In fraction. For speed, we used a shorter NW and the geometry was reduced to a quarter of the NW due to the symmetry (Fig. 1a). FEM model was set-up by assigning boundary and initial conditions; afterwards the steady-state solution was found by the software. Most commercial FEM software packages for continuum mechanics do not have possibilities to describe crystal lattices or misfit dislocations, however usually this can be simulated artificially, using other phenomena, such as thermal expansion etc. In our case we have an InGaN shell, which has larger lattice constants compared with the GaN core. The shell exhibits biaxial compression strain in the planes of the facets in order to avoid creation of the misfit dislocations at the interface and this strain relaxes elastically through entire structure. Using conventional FEM software this can be mimicked by applying initial compression strain, equal to the lattice mismatch so that initially the shell would have the same lattice constant as the core. Then, it is allowed to expand towards the stable state via the free surfaces and deformation of the core. However, this way only elastic relaxation can be simulated, since the shell is not allowed to slip with respect to the core, creating misfit dislocations.

In order to account for the plastic relaxation, which occurs by formation of the misfit dislocations, the core-shell interface was modeled as an infinitely thin elastic layer of a given anisotropic elasticity (or spring constants in different directions) – a feature available in the FEM software. If the virtual spring, coupling the lateral movement between the the core and the shell was infinitely stiff, no slip between core and shell was allowed and only elastic

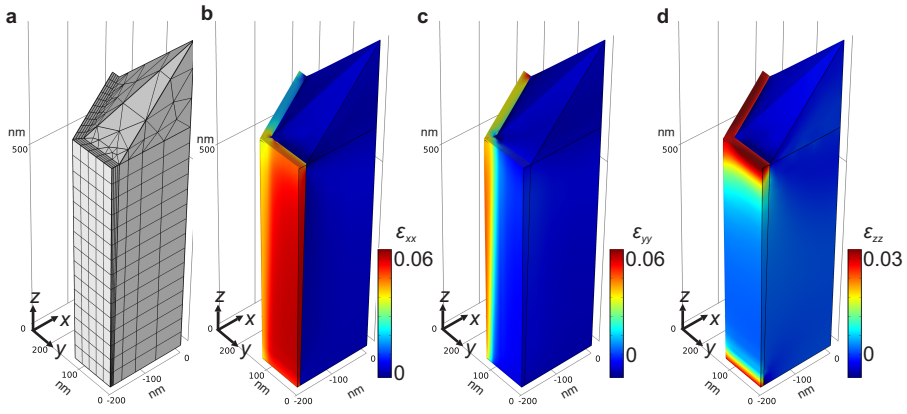

Figure 1: Results of the FEM simulations. a) The model geometry and the mesh. Three normal strain components are shown in b—d.

relaxation was possible, keeping the pseudomorphic relation between the two crystals. On the other hand, loose spring allowed free lateral movement of the shell, fully relaxing the strain via misfit dislocations. Anisotropy of such plastic relaxation can be modeled by simply adjusting two components of the spring constant. Thus, the level of plastic relaxation in $\{1100\}$ and (0001) directions was changed independently. A number of solutions was found by sweeping the parameters of shell composition x and two components of plastic relaxation. The composition of the shell was assumed to be uniform. The solution shown in Fig. 1, was obtained using a model with $x = 0.27$, zero in-plane and 20% axial plastic relaxation of the shell. As we can see from Fig. 1c strain in the shell along the width of the facet is uniform and close to zero in the larger part of the facets. Increased relaxation takes place only in close vicinity of the edges.

In the next step we calculated the scattered intensity distribution around the Bragg peaks using the simulated displacement fields $\mathbf{u}$. Scattered intensity around the peak $\mathbf{h}$ was calculated using the following expression:

$$I_{NW}(\mathbf{Q}) = |FFT(s(\mathbf{r})e^{-i\mathbf{h}\cdot\mathbf{u}(\mathbf{r})})|^2, \tag{1}$$

where $s(\mathbf{r})$ is the shape function. However, intensities simulated for one nanowire cannot be directly compared to the measured on the ensemble due to several reasons. First, the measurements contain contributions from the substrate, containing high defect density, which is not included in our simulations. Second, the measurements were done on an ensemble of nanowires with slightly varying geometry and composition, having random tilts and twists, which blur out any coherence effects and give rise to Debye-Scherrer rings. Some effect of tilting and twisting can be implemented by adding a range of slightly rotated intensity maps. However in order to find average

composition and strain in the shell, it is sufficient to reproduce the peak positions.

2D reciprocal space maps were calculated for both in-plane and out-of-plane slices of the displacement field and compared with the measured reciprocal space maps in Q_xQ_y and Q_xQ_z planes, respectively. The InGaN regions from simulations and measurements were isolated using a mask and the least squares fitting was performed by changing the FEM model. Optimal solution was found by simultaneous fitting of 5 different Bragg peaks. Results of the fitting are summarized in Fig. 2. In the top row we can see the displacement fields obtained from the FEM simulations of the sample with 9 nm thick shell. Panels on the left and right sides show in-plane and out-of-plane cross-sections respectively. In the following rows we can see simulated and measured Bragg peaks side by side. Apart from the weaker diffuse scattering, there is a very good match between the simulations and measurements, especially comparing the positions of the InGaN peaks.

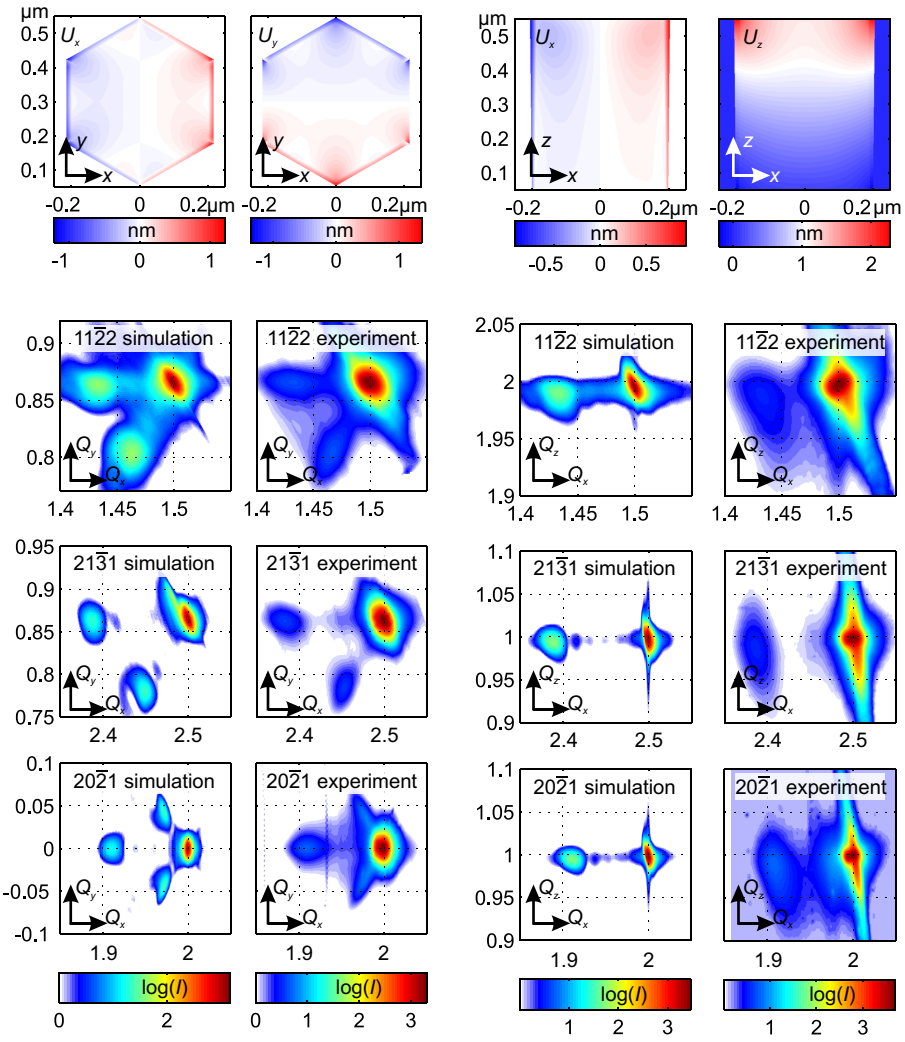

Figure 2: Summary of the XRD simulations. Displacement fields obtained from the FEM simulations are shown in the top row. Following rows show the simulated and measured Bragg peaks side by side. The solutions were obtained for the sample with 9 nm nominal shell thickness, $x_{\mathrm{In}} = 0.27$, $R_{xx} = 0$, $R_{zz} = 0.20$.